BIOCHEMISTRY
including biophysical chemistry & molecular biology

Article

pubs.acs.org/biochemistry

Analysis of High-Affinity Binding of Protein Kinase R to Double-Stranded RNA

Bushra Husain,[†] Ishita Mukerji,[‡] and James L. Cole*[,†,§]

[†]Department of Molecular and Cell Biology, University of Connecticut, Storrs, Connecticut 06269, United States

[‡]Department of Molecular Biology and Biochemistry, Wesleyan University, Middletown, Connecticut 06459, United States

[§]Department of Chemistry and National Analytical Ultracentrifugation Facility, University of Connecticut, Storrs, Connecticut 06269, United States

Supporting Information

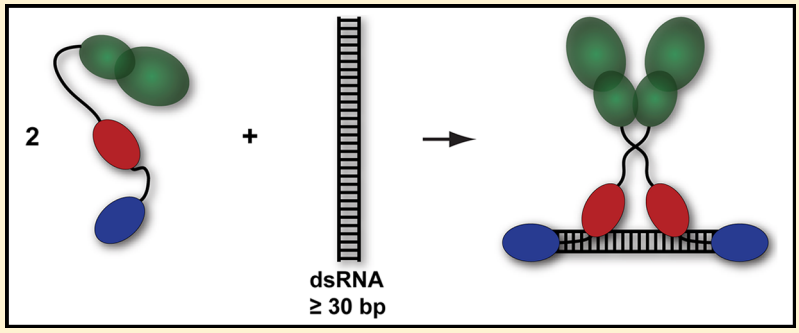

ABSTRACT: Protein kinase R (PKR) is an interferon-induced kinase that plays a pivotal role in the innate immunity response to viral infection. PKR is activated upon binding to double-stranded RNA (dsRNA). Our previous analysis of binding of PKR to dsRNAs ranging from 20 to 40 bp supports a dimerization model for activation in which 30 bp represents the minimal length required to bind two PKR monomers and activate PKR via autophosphorylation. These studies were complicated by the formation of protein−RNA aggregates, particularly at low salt concentrations using longer dsRNAs. Here, we have taken advantage of the enhanced sensitivity afforded using fluorescence-detected analytical ultracentrifugation to reduce the RNA concentrations from micromolar to nanomolar. Under these conditions, we are able to characterize high-affinity binding of PKR to longer dsRNAs in 75 mM NaCl. The PKR binding stoichiometries are increased at lower salt concentrations but remain lower than those previously obtained for the dsRNA binding domain. The dependence of the limiting PKR binding stoichiometries on dsRNA length does not conform to standard models for nonspecific binding and suggests that binding to longer sequences occurs via a different binding mode with a larger site size. Although dimerization plays a key role in the PKR activation mechanism, the ability of shorter dsRNAs to bind two PKR monomers is not sufficient to induce autophosphorylation. We propose that activation of PKR by longer RNAs is correlated with an alternative binding mode in which both of the dsRNA binding motifs contact the RNA, inducing PKR to dimerize via a direct interaction of the kinase domains.

Protein kinase R (PKR) is an important component of the interferon-induced innate immune pathway.[1] PKR is synthesized in the cell in a latent, unphosphorylated form. It becomes activated and undergoes autophosphorylation upon binding to certain host- or pathogen-associated RNAs or upon interacting with the protein PACT. Activated PKR phosphorylates eukaryotic initiation factor 2α (eIF2α), causing an inhibition of protein synthesis. Many viruses have developed mechanisms to inhibit PKR.[2]

PKR contains an N-terminal double-stranded RNA (dsRNA) binding domain and a C-terminal kinase domain, separated by a flexible linker region. The N-terminal dsRNA binding domain (dsRBD) corresponds to the regulatory domain that consists of two tandem copies of the dsRNA binding motif, dsRBM1 and dsRBM2. This motif binds duplex RNA in a non-sequence specific manner but discriminates against single-stranded RNA (ssRNA) and dsDNA.[3] Each motif adopts the conserved $\alpha\beta\beta\beta\alpha$ fold,[4] and they are separated by an unstructured linker of ∼20 amino acids. The crystal structure of a dsRNA binding domain complexed with dsRNA reveals a site size of 16 bp.[5] The C-terminal kinase domain is the catalytic center. The crystal structure of the PKR kinase domain in complex with eIF2α reveals that the catalytic center has the canonical protein kinase fold. The complex forms a dimer where the interface is in the N-terminal lobe of the kinase domain.[6]

PKR is regulated by a variety of cellular and viral RNAs that contain duplex regions.[7] The most well characterized activators of PKR are simple dsRNAs. There is strong evidence that

Received: September 9, 2012
Revised: October 9, 2012
Published: October 12, 2012

dx.doi.org/10.1021/bi301226h | *Biochemistry* 2012, 51, 8764−8770

dimerization plays a crucial role in the mechanism of activation of PKR by dsRNA.[8,9] Latent PKR dimerizes weakly in solution, but this reaction is sufficient to activate PKR in the absence of RNA.[10] An allosteric pathway has been identified that couples the dimer interface with the kinase active site, and dimer interface mutations can modulate PKR activation.[6,11] A hallmark of activation of PKR by dsRNA is the "bell-shaped" curve where low RNA concentrations activate but higher concentrations are inhibitory.[12,13] These observations support a model in which multiple PKRs assemble on a single dsRNA and high dsRNA concentrations dilute PKR monomers onto separate molecules of dsRNA.[14] In the context of regular duplex RNA, a minimum of 30−33 bp of dsRNA is required to activate PKR autophosphorylation and the maximal level of activation increases with duplex length.[13,15]

The mechanism of assembly of PKR on duplex RNAs has been extensively investigated. PKR can bind to duplexes as short as 16−18 bp.[16,17] As expected for a non-sequence specific interaction, the binding stoichiometry increases with dsRNA length.[13,15−18] The binding stoichiometries for dsRBM1 and for a construct containing dsRBM1 and dsRBM2 are greater than those predicted from the site size.[17,19] On the basis of these results, we proposed an overlapping ligand binding model in which the motif binds to multiple faces of the dsRNA duplex and overlaps along the helical axis. The increase in binding affinity with an increasing dsRNA length can be understood as a statistical consequence of the greater number of configurations available on the longer lattice. The intrinsic binding affinities of a dsRBM1−dsRBM2 construct and full-length PKR for a 20 bp RNA are similar,[15,17] but the stoichiometries are lower for the latter. A minimum of 30 bp of dsRNA is required to bind two full-length PKR monomers with high affinity, which correlates with the minimal dsRNA capable of activating through autophosphorylation. Binding affinities increase dramatically when the salt concentration is reduced from 200 to 75 mM NaCl, and a second PKR can bind to 20 bp duplex at lower salt concentrations.[15]

The non-sequence specific interactions of PKR with RNAs are labile, and it is important to use solution biophysical methods to accurately measure the binding parameters at thermodynamic equilibrium. Our previous analyses of binding of PKR to dsRNA by sedimentation velocity analytical ultracentrifugation[10,15] were limited by the formation of nonspecific aggregates, even at the minimal RNA concentrations required for detection using absorption optics. Aggregation is enhanced for longer RNAs and at lower salt concentrations. In addition, it is difficult to quantify high-affinity binding constants because of the limited sensitivity of the absorbance optics. Here, we have used fluorescence detection of labeled dsRNAs to enhance the sensitivity of sedimentation velocity measurements and directly characterize the interaction of PKR with duplex RNAs ranging from 20 to 40 bp at multiple salt concentrations. The binding affinities increase at lower salt concentrations and with longer dsRNAs, and in some cases, the stoichiometries of binding of PKR to dsRNA increase at 75 mM NaCl. The dependence of the binding stoichiometries on dsRNA length does not conform to standard statistical models for nonspecific binding. We propose a model in which the activation of PKR by longer RNAs is correlated with an alternative binding mode that allows for direct interaction of the kinase domains.

EXPERIMENTAL PROCEDURES

All reagents purchased were of reagent grade. Wild-type PKR was expressed and purified as described previously,[10] with the dsRNA affinity column replaced with a hydroxyapatite column.[20] Just before being used, PKR was chromatographed on a Superdex 200 size exclusion column equilibrated in AU200 buffer [20 mM HEPES, 200 mM NaCl, 0.1 mM EDTA, and 0.1 mM TCEP (pH 7.5)]. When required, the protein was buffer exchanged into AU75 (20 mM HEPES, 75 mM NaCl, 0.1 mM EDTA, and 0.1 mM TCEP) using spin columns packed with Bio-gel P-6 (Bio-Rad). The oligoribonucleotides were obtained from Dharmacon (Lafayette, CO) with one strand containing a 5′-fluorescein label. The complementary strands were annealed at 80 °C for 5 min in either AU200 or AU75 and slowly cooled to room temperature before being used. Sedimentation velocity analysis was used to ensure that the dsRNAs were homogeneous (see below).

Quantitative phosphorylation assays were conducted as previously described[10] by incubating 200 nM PKR with varying concentrations of dsRNA in AU75 buffer containing 5 mM $MgCl_2$ and 0.1 mM TCEP at 32 °C for 20 min. The phosphorylation reactions were initiated with 0.4 mM ATP containing 4 μCi of [γ-^{32}P]ATP in each reaction mixture and were quenched after 20 min by adding SDS sample loading buffer. The reaction mixtures were then heated to 90 °C for 3 min and were analyzed using sodium dodecyl sulfate−polyacrylamide gel electrophoresis (SDS−PAGE) and phosphor imaging (Typhoon, GE Healthcare).

Sedimentation velocity experiments were performed using a Beckman-Coulter XL-I analytical ultracentrifuge equipped with an AU-FDS fluorescence detector (AVIV Biomedical, Lakewood, NJ) at 20 °C and 40000 rpm. Samples contained 20−30 nM dsRNA, and varying concentrations of PKR in either AU200 or AU75 buffer were loaded into double-sector cells equipped with 1.2 cm Spin60 charcoal-Epon centerpieces (Spin Analytical, Berwick, ME) and quartz windows. During a prerun at 5000 rpm, the photomultiplier voltage and gain multiplier settings were adjusted to give ∼3000 counts and the focus depth was set to give a maximal signal. Absorbance intensity scans were recorded for each channel following the sedimentation velocity experiment, and the position of the meniscus was determined from a characteristic downward intensity spike. Although it has recently been asserted that the fluorescence detector produces nonlinear responses and underestimates sedimentation coefficients,[21] we have found that the detector produces linear responses up to 500 nM and the sedimentation coefficients agree with those determined by absorbance detection (J. W. Lary, B. Husain, and J. L. Cole, manuscript in preparation).

The protein partial specific volume and the buffer densities and viscosities were calculated using SEDNTERP.[22] The partial specific volumes of the dsRNAs were fixed at 0.55 mL g^{-1}. The sedimentation velocity data for the dsRNAs were first analyzed using a $c(s)$ distribution model with Sedfit[23] to ensure that the preparations were homogeneous and free of contaminants. The data were then fit to a single-species model to obtain the sedimentation coefficients and the buoyant molar masses that were then fixed in subsequent global analyses of PKR binding. Sedimentation velocity analyses of PKR−dsRNA interactions were performed as previously described,[24] with some modifications to accommodate fluorescence data as described below. Initially, the data were analyzed using the time derivative

dx.doi.org/10.1021/bi301226h | Biochemistry 2012, 51, 8764−8770

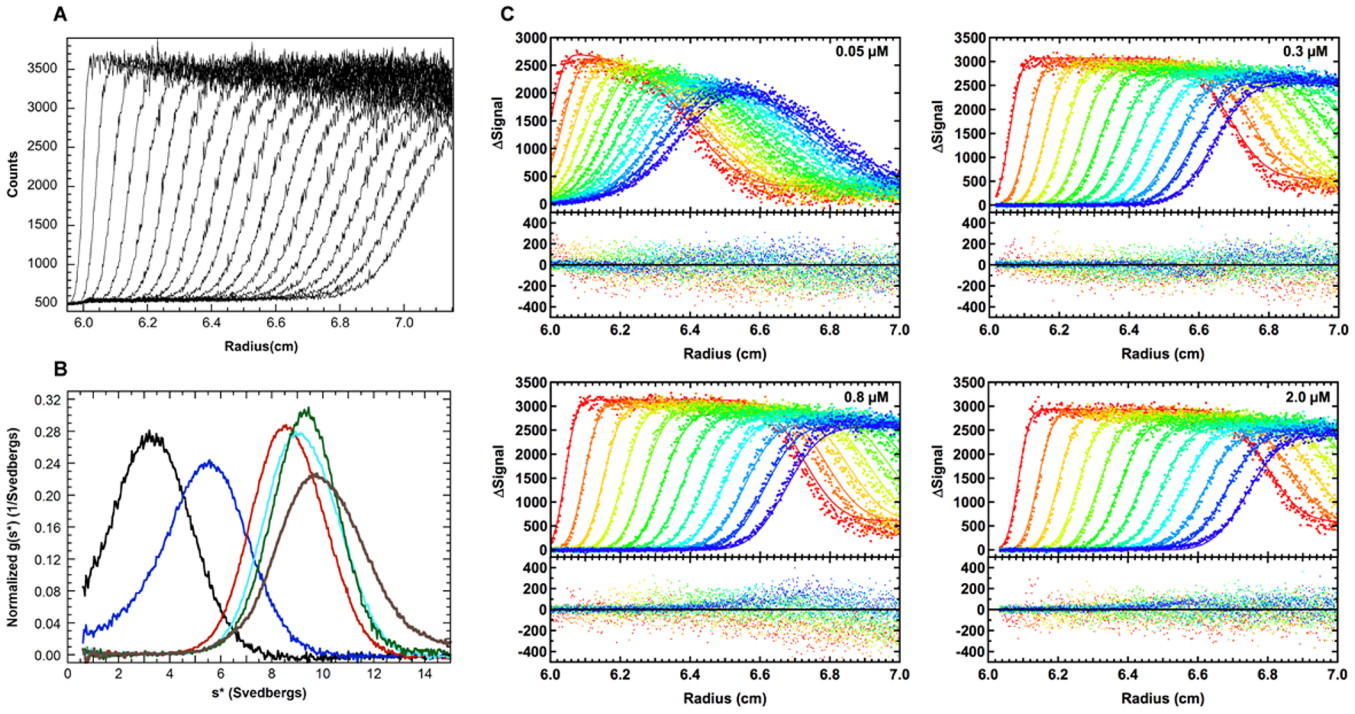

Figure 1. Sedimentation velocity analysis of binding of PKR to a 40 bp dsRNA in AU75. (A) Raw sedimentation velocity profiles for 40 bp dsRNA. For the sake of clarity, only every 13th scan is shown. (B) Normalized $g(s^*)$ distributions of 0.03 μM 40 bp dsRNA (black), dsRNA with 0.05 μM PKR (blue), dsRNA with 0.3 μM PKR (red), dsRNA with 0.8 μM PKR (cyan), dsRNA with 2 μM PKR (green), and dsRNA with 7 μM PKR (brown). (C) Global analysis of difference curves. The data were subtracted in pairs to remove systematic noise, and the four data sets at the PKR concentrations were fit to a 2:1 binding model using SEDANAL.[27] The top panels show the data (points) and fit (solid lines) and the bottom panels the residuals (points). The best-fit parameters are listed in Table 1. For the sake of clarity, only every 7th difference curve of the 165 scans that were fit is shown.

method[25] with DCDT+[26] to obtain $g(s^*)$ distributions to define the interaction model. Model dependent global analysis was performed using SEDANAL[27] to define the association constants and sedimentation coefficients of the protein−RNA complexes. For data acquired with the fluorescence detector, the amplitude of the stochastic noise depends strongly on the signal intensity. Therefore, the curve fits were weighted by the standard deviation at each point. This also served to convert the rmsd reported by SEDANAL from arbitrary fluorescence intensity units to χ, where a value of 1.0 corresponds to a perfect fit. Joint confidence intervals were obtained using the F statistic to define a statistically significant increase in the variance.

RESULTS

The enhanced sensitivity of fluorescence detection in sedimentation velocity measurements allows the dsRNA concentrations to be greatly reduced, from ~1 μM using absorbance detection at 260 nm to 20−30 nM for fluorescence analysis of 5′-fluorescein-labeled RNAs. Figure 1 shows an analysis of binding of PKR to dsRNA using a long sequence (40 bp) at a low salt concentration (75 mM NaCl), conditions that previously were found to promote aggregation. The signal/noise ratio of the raw sedimentation velocity traces for the RNA alone is excellent (Figure 1A). The data fit well to a model of a single species with a corrected sedimentation coefficient ($s_{20,w}$) of 3.69 S and a molecular weight of 30979, consistent with a predicted molecular weight of 26128 based on the RNA sequence (Table S1, Supporting Information). Thus, this dsRNA preparation is homogeneous and suitable for analysis of PKR binding.

The binding of PKR to the 40 bp dsRNA was characterized by a sedimentation velocity titration using fluorescence detection. Although the general approach is similar to the method we have previously described by analysis of PKR−RNA interactions using absorbance detection,[24] the RNA concentration here is much lower and we are able to access a much broader range of PKR concentrations (from nanomolar to micromolar). Another difference is that the PKR contributes, albeit weakly, to the absorbance signal measured at 260 nm, whereas only the fluorescein-labeled RNA contributes to the fluorescence signal.

Initially, the velocity data were analyzed using a model-independent approach to help define the correct binding mode. Figure 1B shows a titration of the 40 bp dsRNA over a broad range of PKR concentrations from 50 nM to 7 μM, represented as an overlay of normalized $g(s^*)$ sedimentation coefficient distributions. The formation of PKR−dsRNA complexes causes the distributions to shift far to the right, to a saturating value of ~9.46 S at 2 μM PKR. Hydrodynamic calculations indicate that the magnitude of this shift is greater than that expected for binding of a single PKR but is consistent with binding of three PKR monomers (Table S1, Supporting Information). The $g(s^*)$ distribution at 7 μM exhibits a shoulder at higher coefficient values, indicating formation of higher-order aggregates. However, the data obtained over the range from 50 nM to 2 μM can be globally fit to a sequential binding model to resolve the three equilibrium constants (Figure 1C). The fit is of good quality, with small systematic deviations in the residuals and an rmsd of 1.70. As we have previously

dx.doi.org/10.1021/bi301226h | Biochemistry 2012, 51, 8764−8770

Table 1. PKR−dsRNA Dissociation Constants Measured in AU75 and AU200 Buffers at 20 °C[a]

dsRNA (bp)	[NaCl] (mM)	model[b]	K_{d1} (nM)	K_{d2} (nM)	K_{d3} (nM)	rmsd[c]
20	75	2	45.2 (35.2, 59.5)	54.1 (40.9, 69.9)	–	1.54
20	200	1	303 (263, 349)	–	–	1.50
25	75	2	7.8 (6.8, 9.0)	473 (391, 572)	–	1.83
25	200	1	438 (380, 497)	–	–	1.27
30	75	2	100.1 (83.1, 122.5)	22.6 (18.6, 26.8)	–	1.54
30	200	2	52.0 (46.0, 58.3)	6270 (3920, 11800)	–	1.31
35	75	2	7.6 (6.7, 8.6)	69.1 (50.8, 95.2)	–	1.67
35	200	2	61.1 (47.9, 72.8)	4910 (2950, 8260)		1.38
40	75	3	32.1 (27.3, 38.0)	52.4 (40.6, 67.8)	245 (212, 280)	1.70
40	200	2	38.1 (29.5, 47.3)	813 (645, 1070)	–	1.52

[a]Parameters were obtained by global nonlinear least-squares analysis of sedimentation velocity experiments. The values in parentheses represent the 95% joint confidence intervals obtained using the *F* statistic. [b]The model is specified by the stoichiometry of PKR binding. [c]The root-mean-square deviation of the fit. Because the fits were weighted by the standard deviation of the data at each point, a perfect fit corresponds to an rmsd of unity.

observed for binding of PKR to dsRNA lattices,[15,17,19] the first PKR binds most strongly, with a K_{d1} of ∼30 nM, and the second and third ligands bind progressively more weakly, with a K_{d2} of ∼50 nM and a K_{d3} of ∼ 250 nM (Table 1). Note that these are stepwise, macroscopic dissociation constants and are not corrected for statistical effects. Fitted values for the sedimentation coefficients of the RNA−PKR, RNA−PKR_2, and RNA−PKR_3 complexes (Table S1, Supporting Information) correspond to frictional ratios of 1.42, 1.46, and 1.40, respectively, which lie in the range typically observed for RNA−PKR complexes.[24]

These results obtained with the 40 bp dsRNA in AU75 demonstrate that it is feasible to analyze binding of PKR to relatively long dsRNAs, even at low ionic strengths, by reducing the dsRNA concentration into the nanomolar range using the high sensitivity afforded by fluorescence-detected analytical ultracentrifugation. We have employed this approach to rigorously define the PKR binding stoichiometries and affinities for a truncation series of dsRNAs ranging from 20 to 40 bp in 5 bp increments. Binding parameters were obtained at both high (200 mM) and low (75 mM) NaCl concentrations. As described above for the 40 bp duplex, the binding stoichiometries were based on the limiting sedimentation coefficients estimated from the shift in $g(s^*)$ distributions with increasing PKR concentrations. The models were verified, and binding constants were resolved by global analysis of the data using SEDANAL. For the measurements performed in 75 mM NaCl, where the binding affinity is high, it was not possible to reliably fit the sedimentation coefficients of the intermediate dsRNA−PKR complexes because of the low population of these species. The sedimentation coefficients for these species were fixed at the values obtained in 200 mM NaCl (corrected for buffer density and viscosity). The results of the fits are summarized in Table 1, and the corresponding hydrodynamic parameters are listed in Table S1 of the Supporting Information.

There are several trends that emerge from the analysis of binding of PKR to the RNA truncation series under high- and low-salt conditions. For several of the dsRNAs (20, 25, and 40 bp), the apparent binding stoichiometries increase at lower salt concentrations. This effect is likely associated with the enhancement of binding affinity that occurs at lower salt concentrations.[16] The K_d values decrease by as much as 10-fold upon reduction of the NaCl concentration from 200 to 75 mM. Thus, the second (20 and 25 bp) or third (40 bp) PKR cannot be detected at high salt concentrations because K_d becomes too high. In most cases, the dissociation constants sequentially increase such that $K_{d1} < K_{d2} < K_{d3}$. This successive decrease in binding affinities is not due to a negative cooperativity but represents a statistical effect. The macroscopic, stepwise binding constants measured in sedimentation velocity experiments correspond to the product of an intrinsic binding constant *k* and a statistical factor corresponding to the number of microscopic configurations of the ligand on the dsRNA.[19,28] As the RNA is sequentially saturated with ligand, the statistical factors decrease, resulting in successively weaker binding. As expected for a nonspecific protein−nucleic acid interaction, the limiting binding stoichiometries measured in AU75 increase with the length of the dsRNA. However, this trend is surprisingly weak: when the lattice length is doubled from 20 to 40 bp, the number of PKRs that bind does not double and increases only from 2 to 3.

It has previously been reported that activation of PKR requires a minimum of 30 bp of dsRNA,[13] and we have correlated PKR activation with the stoichiometry of binding measured in AU200 buffer for the dsRNA truncation series.[15] Our PKR binding data indicate a strong dependence of binding stoichiometry on salt concentration. Thus, we have re-examined the dependence of PKR activation on dsRNA length in a lower-salt buffer, AU75 (Figure 2). The activation profiles are very similar to those we previously observed at higher salt concentrations. A minimum of 30 bp is required to detect activation with a maximum near 30 nM, and the maximal extent of activation increases with the length of the dsRNA. Thus, although the 20 and 25 bp dsRNAs can each bind two PKRs in AU75 buffer, they are incapable of stimulating autophosphorylation under the same conditions.

DISCUSSION

The enhanced sensitivity afforded using fluorescein-tagged dsRNAs with fluorescence-detected analytical ultracentrifugation has allowed to us greatly reduce RNA concentrations from micromolar to nanomolar. In contrast to previous studies of PKR−dsRNA interactions by analytical ultracentrifugation,[15] at lower RNA concentrations the analysis of binding stoichiometries and affinities is not complicated by aggregation formation, and we were able to directly characterize the interaction of PKR with duplex RNAs ranging from 20 to 40 bp at multiple salt concentrations. The binding stoichiometries obtained here at 200 mM NaCl agree with those obtained earlier except for that of the 40 bp dsRNA, for which we previously detected three PKR ligands by fluorescence anisotropy and sedimentation

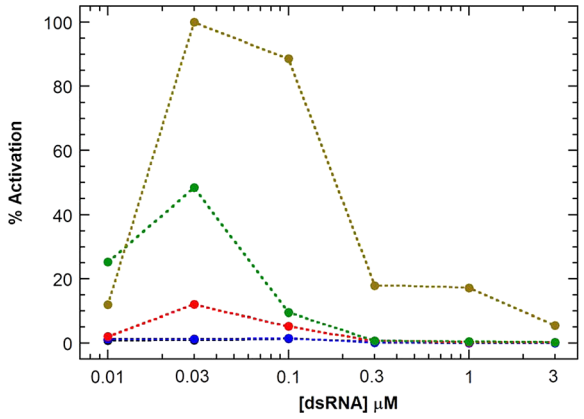

Figure 2. Activation of PKR by varying-length duplex RNAs in 75 mM NaCl. Experiments were performed as previously described[10] in AU75 buffer at 32 °C. Each reaction mixture contained 200 nM PKR, 0.4 mM ATP, 4 μCi of [γ-^{32}P]ATP, and the indicated amount of RNA. The reaction was allowed to proceed for 20 min at 32 °C before being quenched with SDS loading buffer and the mixture resolved via SDS–PAGE: 20 bp dsRNA (black), 25 bp dsRNA (blue), 30 bp dsRNA (red), 35 bp dsRNA (green), and 40 bp dsRNA (brown).

equilibrium[15] but only two in the present sedimentation velocity measurements. Note that sedimentation velocity has greater resolving power than the earlier techniques, and small amounts of the aggregate may have contributed to a higher apparent stoichiometry. The dissociation constants for the 20 and 30 bp dsRNAs in 200 mM NaCl differ slightly from those previously obtained using absorbance detection. The origin of the discrepancies is not clear, but the broader PKR concentration range used for these experiments makes them more reliable.

The dependence of PKR binding stoichiometries and affinities on salt concentration and RNA length provides insight into the mechanism of assembly of PKR on duplex RNAs and formation of active complexes. There is a large electrostatic component to the PKR–dsRNA interaction[16] that results in increased binding affinity as the NaCl concentration is decreased from 200 to 75 mM. The concomitant increase in binding stoichiometries for several of the RNAs is likely associated with the enhancement of binding affinity. The limited solubility of PKR–RNA complexes precludes measurements at NaCl concentrations below 75 mM, and we make the assumption that the stoichiometries measured under these conditions correspond to the maximum. We have previously

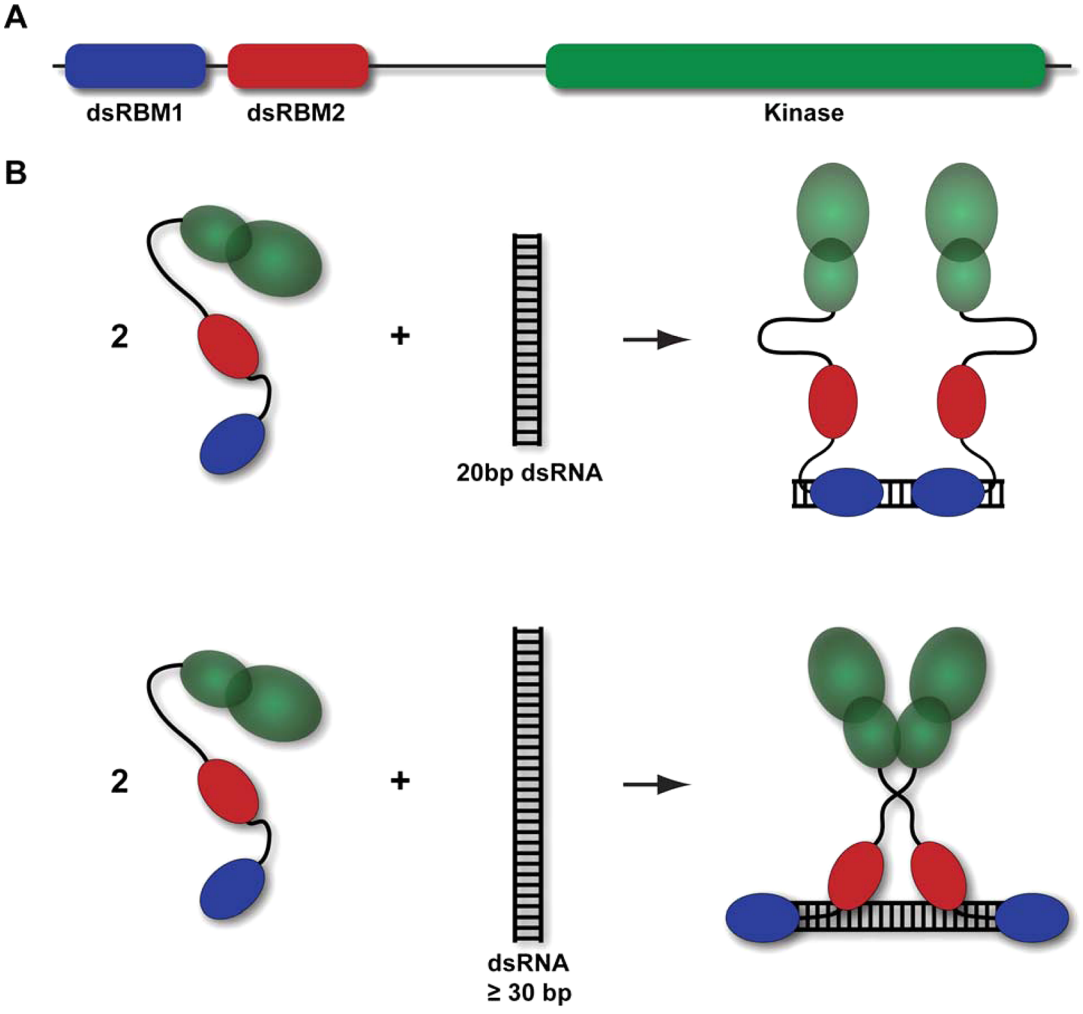

Figure 3. Model for binding of PKR to short and long dsRNAs. (A) Domain organization of PKR. (B) Two PKRs are able to bind to the 20 bp dsRNA at low salt concentrations via dsRBM1. PKR binds to dsRNAs of ≥30 bp with a larger site size via interaction of both dsRBM1 and dsRBM2. This binding model facilitates dimerization of the kinase domains, resulting in PKR activation.

dx.doi.org/10.1021/bi301226h | *Biochemistry* 2012, 51, 8764–8770

characterized the binding of the PKR dsRBD, containing both dsRBM1 and dsRBM2, and dsRBM1 alone to the same dsRNA truncation series in AU75 buffer.[17,19] The stoichiometries for the full-length enzyme are consistently lower than for either domain construct across the range of RNA lengths. Presumably, the presence of the kinase domain and linker in PKR results in steric hindrance that increases the effective binding site size relative to the domain constructs.

The dependence of the limiting PKR binding stoichiometries on dsRNA length does not conform to standard models[29−31] for nonspecific binding of proteins to finite nucleic acid lattices. The stoichiometries are expected to regularly increase with RNA length, but for PKR, they remain fixed at two PKRs per RNA from 20 to 35 bp and increase only to 3 for the 40 bp sequence. In contrast, the stoichiometries for binding of dsRBM1 to RNA increase strongly with length and conform to a modified overlapping ligand binding model[19] in which the motif binds to multiple faces of the dsRNA duplex and overlaps along the helical axis with a site size of 12 bp and a minimal overlap of 4 bp.[17] The dsRBD also follows this model for RNAs up to a length of 30 bp but deviates strongly for longer RNAs, and the stoichiometries actually decrease between 35 and 40 bp. These data indicate a change in the mode of binding to a larger site size with increasing RNA length. This model is supported by NMR mapping experiments showing that only the N-terminus of dsRBM2 interacts with a 20 bp dsRNA, but extensive interactions are observed upon binding to the 40 bp sequence.[17] In addition, affinity cleavage experiments demonstrate that simultaneous binding of both dsRBMs of PKR is correlated with PKR activation.[32] We suggest that an analogous change in binding mode occurs as a function of RNA length for the full-length enzyme, resulting in an increase in the site size and a constant binding stoichiometry from 20 to 35 bp.

Although dimerization clearly plays a critical role in the PKR activation mechanism,[8] the ability of a single dsRNA to bind two PKR monomers is not sufficient to induce autophosphorylation. In AU75 buffer, the 20 and 25 bp RNAs each bind two PKRs yet are incapable of inducing measurable autophosphorylation (Figure 2). Previously, we suggested that the inability of these shorter RNAs to be activated in AU200 is associated with low binding affinities, resulting in a small population of the active PKR_2−RNA species.[15] However, the 20 and 25 bp RNAs also are not activated in AU75, yet the binding affinities measured in this buffer are as strong as those measured for a 30 bp RNA in AU200 where this RNA is capable of activating PKR autophosphorylation. Thus, additional factors must be limiting the ability of short RNAs to induce the functional, active dimeric form of PKR. We propose that activation of PKR by longer RNAs requires a binding mode that is inaccessible upon binding to shorter RNAs (Figure 3). Our RNA binding data indicate that this active binding state is characterized by a larger size. Possibly, this mode is required to allow for direct interaction of the kinase domains to mediate functional dimerization. Experiments are now underway to directly test this hypothesis.

■ ASSOCIATED CONTENT

Supporting Information

Hydrodynamic parameters for dsRNAs and dsRNA−PKR complexes (Table S1). This material is available free of charge via the Internet at http://pubs.acs.org.

■ AUTHOR INFORMATION

Corresponding Author

*Department of Molecular and Cell Biology, 91 N. Eagleville Rd., U-3125, University of Connecticut, Storrs, CT 06269. Phone: (860) 486-4333. Fax: (860) 486-4331. E-mail: james.cole@uconn.edu.

Funding

This work was supported by National Institutes of Health Grant AI-53615 J.L.C.

Notes

The authors declare no competing financial interest.

■ ABBREVIATIONS

dsRBD, dsRNA binding domain; dsRBM, dsRNA binding motif; eIF2α, eukaryotic initiation factor 2α; PKR, RNA-activated protein kinase; rmsd, root-mean-square deviation.

■ REFERENCES

(1) Toth, A. M., Zhang, P., Das, S., George, C. X., and Samuel, C. E. (2006) Interferon action and the double-stranded RNA-dependent enzymes ADAR1 adenosine deaminase and PKR protein kinase. *Prog. Nucleic Acid Res. Mol. Biol. 81*, 369−434.

(2) Langland, J. O., Cameron, J. M., Heck, M. C., Jancovich, J. K., and Jacobs, B. L. (2006) Inhibition of PKR by RNA and DNA viruses. *Virus Res. 119*, 100−110.

(3) Tian, B., Bevilacqua, P. C., Diegelman-Parente, A., and Mathews, M. B. (2004) The double-stranded-RNA-binding motif: Interference and much more. *Nat. Rev. Mol. Cell Biol. 5*, 1013−1023.

(4) Nanduri, S., Carpick, B. W., Yang, Y., Williams, B. R., and Qin, J. (1998) Structure of the double-stranded RNA binding domain of the protein kinase PKR reveals the molecular basis of its dsRNA-mediated activation. *EMBO J. 17*, 5458−5465.

(5) Ryter, J. M., and Schultz, S. C. (1998) Molecular basis of double-stranded RNA-protein interactions: Structure of a dsRNA-binding domain complexed with dsRNA. *EMBO J. 17*, 7505−7513.

(6) Dar, A., Dever, T., and Sicheri, F. (2005) Higher-Order Substrate Recognition of eIF2α by the RNA-Dependent Protein Kinase PKR. *Cell 122*, 887−900.

(7) Nallagatla, S. R., Toroney, R., and Bevilacqua, P. C. (2011) Regulation of innate immunity through RNA structure and the protein kinase PKR. *Curr. Opin. Struct. Biol. 21*, 119−127.

(8) Cole, J. L. (2007) Activation of PKR: An open and shut case? *Trends Biochem. Sci. 32*, 57−62.

(9) Robertson, H. D., and Mathews, M. B. (1996) The regulation of the protein kinase PKR by RNA. *Biochimie 78*, 909−914.

(10) Lemaire, P. A., Lary, J., and Cole, J. L. (2005) Mechanism of PKR activation: Dimerization and kinase activation in the absence of double-stranded RNA. *J. Mol. Biol. 345*, 81−90.

(11) Dey, M., Cao, C., Dar, A. C., Tamura, T., Ozato, K., Sicheri, F., and Dever, T. E. (2005) Mechanistic link between PKR dimerization, autophosphorylation, and eIF2α substrate recognition. *Cell 122*, 901−913.

(12) Hunter, T., Hunt, T., Jackson, R. J., and Robertson, H. D. (1975) The characteristics of inhibition of protein synthesis by double-stranded ribonucleic acid in reticulocyte lysates. *J. Biol. Chem. 250*, 409−417.

(13) Manche, L., Green, S. R., Schmedt, C., and Mathews, M. B. (1992) Interactions between double-stranded RNA regulators and the protein kinase DAI. *Mol. Cell. Biol. 12*, 5238−5248.

(14) Kostura, M., and Mathews, M. B. (1989) Purification and activation of the double-stranded RNA-dependent eIF-2 kinase DAI. *Mol. Cell. Biol. 9*, 1576−1586.

(15) Lemaire, P. A., Anderson, E., Lary, J., and Cole, J. L. (2008) Mechanism of PKR Activation by dsRNA. *J. Mol. Biol. 381*, 351−360.

(16) Bevilacqua, P. C., and Cech, T. R. (1996) Minor-groove recognition of double-stranded RNA by the double-stranded RNA-

binding domain from the RNA-activated protein kinase PKR. *Biochemistry 35*, 9983−9994.
(17) Ucci, J. W., Kobayashi, Y., Choi, G., Alexandrescu, A. T., and Cole, J. L. (2007) Mechanism of interaction of the double-stranded RNA (dsRNA) binding domain of protein kinase R with short dsRNA sequences. *Biochemistry 46*, 55−65.
(18) Schmedt, C., Green, S. R., Manche, L., Taylor, D. R., Ma, Y., and Mathews, M. B. (1995) Functional characterization of the RNA-binding domain and motif of the double-stranded RNA-dependent protein kinase DAI (PKR). *J. Mol. Biol. 249*, 29−44.
(19) Ucci, J. W., and Cole, J. L. (2004) Global analysis of non-specific protein-nucleic interactions by sedimentation equilibrium. *Biophys. Chem. 108*, 127−140.
(20) Anderson, E., Pierre-Louis, W. S., Wong, C. J., Lary, J. W., and Cole, J. L. (2011) Heparin Activates PKR by Inducing Dimerization. *J. Mol. Biol. 413*, 973−984.
(21) Zhao, H., Berger, A. J., Brown, P. H., Kumar, J., Balbo, A., May, C. A., Casillas, E., Laue, T. M., Patterson, G. H., Mayer, M. L., and Schuck, P. (2012) Analysis of high-affinity assembly for AMPA receptor amino-terminal domains. *J. Gen. Physiol. 139*, 371−388.
(22) Harding, S. E., Rowe, A. J., and Horton, J. C., Eds. (1992) Computer-aided interpretation of sedimentation data for proteins. In *Analytical Ultracentrifugation in Biochemistry and Polymer Science*, pp 90−125, Royal Society of Chemistry, Cambridge, England.
(23) Schuck, P. (2000) Size-distribution analysis of macromolecules by sedimentation velocity ultracentrifugation and Lamm equation modeling. *Biophys. J. 78*, 1606−1619.
(24) Wong, C. J., Launer-Felty, K., and Cole, J. L. (2011) Analysis of PKR-RNA interactions by sedimentation velocity. *Methods Enzymol. 488*, 59−79.
(25) Stafford, W. F. (1992) Boundary analysis in sedimentation transport experiments: A procedure for obtaining sedimentation coefficient distributions using the time derivative of the concentration profile. *Anal. Biochem. 203*, 295−301.
(26) Philo, J. S. (2006) Improved methods for fitting sedimentation coefficient distributions derived by time-derivative techniques. *Anal. Biochem. 354*, 238−246.
(27) Stafford, W. F., and Sherwood, P. J. (2004) Analysis of heterologous interacting systems by sedimentation velocity: Curve fitting algorithms for estimation of sedimentation coefficients, equilibrium and kinetic constants. *Biophys. Chem. 108*, 231−243.
(28) Cole, J. L. (2004) Analysis of heterogeneous interactions. *Methods Enzymol. 384*, 212−232.
(29) Epstein, I. R. (1978) Cooperative and non-cooperative binding of large ligands to a finite one-dimensional lattice: A model for ligand-oligonucleotide interactions. *Biophys. Chem. 8*, 327−339.
(30) Latt, S. A., and Sober, H. A. (1967) Protein-nucleic acid interactions. II. Oligopeptide-polyribonucleotide binding studies. *Biochemistry 6*, 3293−3306.
(31) Munro, P. D., Jackson, C. M., and Winzor, D. J. (2000) Consequences of the non-specific binding of a protein to a linear polymer: Reconciliation of stoichiometric and equilibrium titration data for the thrombin-heparin interaction. *J. Theor. Biol. 203*, 407−418.
(32) Spanggord, R. J., Vuyisich, M., and Beal, P. A. (2002) Identification of binding sites for both dsRBMs of PKR on kinase-activating and kinase-inhibiting RNA ligands. *Biochemistry 41*, 4511−4520.